IL NUOVO CIMENTO **47 C** (2024) 256
DOI 10.1393/ncc/i2024-24256-y

COMMUNICATIONS: SIF Congress 2023

Towards dipolar supersolids in a ring

N. PRETI(1)(2)(*)

(1) *Dipartimento di Fisica e Astronomia and LENS, - Florence, Italy*
(2) *CNR-INO, Sezione di Pisa - Pisa, Italy*

received 24 January 2024

Summary. — In recent years many fundamental properties of the supersolid phase of matter have been studied, but the question of how such a peculiar state rotates remains experimentally unexplored. In this paper I report on an ongoing experiment made towards the trapping of a supersolid inside a ring potential, to study its rotational properties. I present both the experimental realization of the ring and numerical simulations done to study the superfluid to supersolid phase transition in an annular geometry.

1. – Introduction

The supersolid is a peculiar phase of matter characterized by the coexistence of superfluidity and a crystal-like structure. Even though this state of matter was predicted to exist more than fifty years ago and the prime candidates for its discovery were quantum crystals like solid helium, the phenomenon of supersolidity was first observed in quantum gases of magnetic atoms [1-3]. A peculiar feature of these gases is given by their excitation spectrum, that shows a local minimum at finite momentum, also called "Roton". This same phenomenon was studied much earlier in liquid helium. In dipolar gases the energy of the rotonic minimum can be tuned by changing the relative importance of contact and dipolar interactions via Feshbach resonances. When the roton's energy crosses zero it becomes favorable for the system to have a macroscopic occupation of the roton's momentum state, thus inducing an instability that leads to the formation of an array of clusters. This instability can then be stabilized by quantum fluctuations. This mechanism is what brings forth supersolidity in strongly magnetic quantum gases. Since its discovery, many characteristic properties of the supersolid have been extensively studied [4-9], but one fundamental superfluid-like property is yet to be observed in supersolids, this being the ability to sustain persistent currents. These excitations are predicted to behave in a very

(*) E-mail: niccolo.preti@unifi.it

distinct manner in supersolids with respect to regular superfluids. A supersolid should in fact be able to rotate at low angular frequencies without excitations of vortices thanks to its crystalline nature, while a jump in angular momentum should still be present for higher velocities but its magnitude is predicted to be reduced from $\hbar$, that is the value for regular superfluids [10]. The study of persistent currents in quantum gases can be achieved using ring-shaped potentials [11-13]. The ring geometry is in fact the simplest realization of periodic boundary conditions that are needed to study currents. In this article I will present the experimental results of my master thesis [14] made towards the realization of a dipolar supersolid of bosonic dysprosium atoms, trapped in a ring potential. In sect. **2** I will report the characterization of a blue laser diode used to realize a repulsive potential for dysprosium atoms. In sect. **3** I will present one method to realize light shaped as a ring using a digital micromirror device. In this section I will also present numerical simulations of the superfluid to supersolid phase transition inside the experimentally realized ring.

2. – Realization of a blue repulsive potential for dysprosium atoms

2˙1. *The light source.* – The source of light that we will implement to realize the ring potential is given by a commercial continuous mode multimode diode laser (Nichia NDV4313) capable of producing up to 120 mW around 404 nm. We want to work with such a short wavelength because the resolution of all lenses has a lower bound given by diffraction that scales linearly with the wavelength. Given this, working with the shortest wavelength possible will allow us to have the best possible resolution when projecting our ring potential on the atoms. The emission spectrum of this light source is extremely close to that of a dysprosium absorption line, which is the $[\mathrm{Xe}]4f^{10}6s^2(^5I_8) \rightarrow [\mathrm{Xe}]4f^{10}(^5I_8)6s6p(1P_1^o)(8,1)_7$. This is a strong dipole-permitted transition with central absorption wavelength 404.7 nm and a natural linewidth of 30 MHz. In fig. 1(a) the bare diode's spectrum is reported for different values of its temperature, which can be adjusted through a Peltier cell placed in thermal contact with the diode. As shown in the picture, the spectrum of the bare diode laser crosses the transition's wavelength for all reachable diode's temperatures. This is a problem for two main reasons: the first one being the fact that all the light that has a wavelength greater than the absorption, one will contribute to an attractive potential and not to a repulsive one. Secondly, the more we close the gap between the laser and absorption frequencies, the more the light scattering rate will grow, eventually diverging when the two match. To not heat up the sample during the interaction with our potential, real scattering processes are to be avoided, which means that it is mandatory that the laser spectrum doesn't cross the transition. To solve this problem we implemented the optical scheme shown in fig. 1(b). The light coming from the diode is first coupled to an extended cavity, making the laser single mode up to an output power of around 20 mW. Another advantage of the extended cavity laser configuration (ECDL) is that, by rotating the diffraction grating, it's possible to tune the laser peak emission wavelength by a couple of nm. To monitor the frequency operation of the diode laser we use a scanning Fabry-Pérot interferometer, characterized by a Free spectral range of 1.5 GHz and a typical finesse of about 250. After exiting from the extended cavity, the light passes through an optical isolator, implemented to avoid having reflection coming back inside the active medium of the laser. Because we work very close to resonance, this first stage of spectral filtering is not enough to have coherent interaction between the laser and the atoms (see sect. **2**˙2). We then implement a second diffraction grating in the system. The first diffraction order exiting this grating

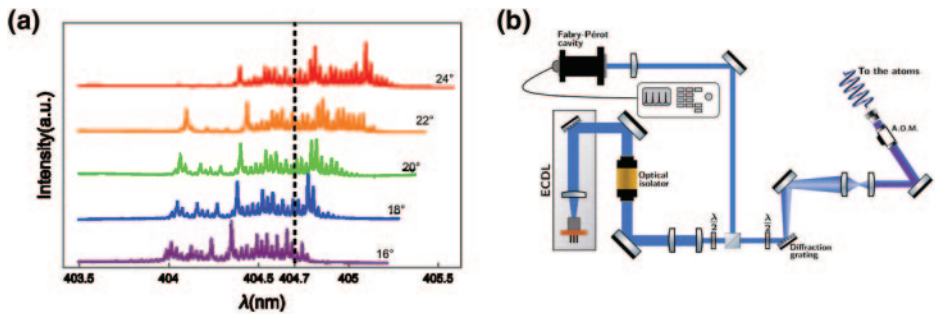

Fig. 1. – (a) Diode laser spectrum for various different temperatures. (b) Sketch of the optical setup implemented to narrow down the laser spectrum.

is coupled to a single mode fiber. Because of this, different wavelengths will impinge on the collimating lens of the fiber in different positions, meaning that wavelengths that are far away enough from the beam center will not get coupled inside the fiber. Consequently, the fiber in this configuration also acts as a frequency filter. An acusto optic modulator (A.O.M.) is also placed in the system to tune the interaction time of the laser with the atoms.

2·2. *Measuring the lifetime of a dysprosium condensate.* – To test if the laser in the setup shown in fig. 1(b) can interact in a coherent way with the atoms, we measure lifetimes of a dysprosium Bose-Einstein condensate (BEC) as a function of the interaction time with the blue light. The BEC is initially trapped in a crossed dipole trap made by two 1064 nm infrared lasers([1]), and the blue laser hits the BEC in a plane that is perpendicular to this crossed trap, directed along the condensate's magnetization $\boldsymbol{M}$, as shown in the inset of fig. 2. This measurement is directly related to the scattering properties of the atom-light interaction since if an atom absorbs a blue photon, it gets a recoil energy of about 360 nK and this is enough to kick it out of the infrared dipole trap. The results for the lifetime with and without the second stage of frequency filtering are shown in fig. 2. Using a fitting function of the form $f(t) = Ae^{-t/\tau}$ it is possible to extract from the data the lifetime τ, defined as the interaction time at which the number of trapped atoms is $1/e$ of the initial number. Without the second grating we obtain a lifetime of (120 ± 30) ms, which is far too short for our purposes. With the second grating the lifetime becomes (2.5 ± 0.3) s. This shows that the setup shown in fig. 1(b) is efficient in removing the on-resonance wavelengths and make them not interact with the atoms. The main challenge of this optical setup is that we make use of two diffractive elements and we also couple the light inside a single mode fiber. At the end of the optical path we can only send about $2-3$ mW of power to the atoms and we can ask ourselves if this will be enough to trap them. Fortunately, the potential for the atom-light interaction not only depends on the intensity of the laser beam, but also on another quantity called atomic polarizability, that in principle should be very high seeing as we are working extremely close to a resonance. Theoretical estimations give a value of about -13000 atomic units for the polarizability at 404.1 nm. This means that we can realize a repulsive potential of 500 nK with just 1 mW of blue light and a waist of 60 μm, with sufficiently long lifetimes.

([1]) More information on the BEC preparation can be found in [1].

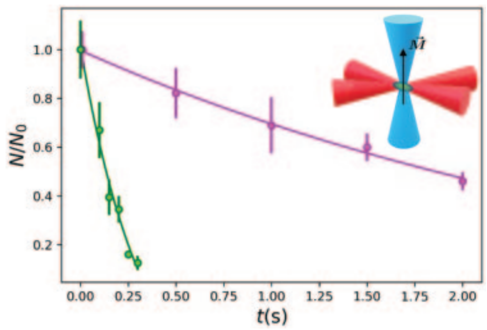

Fig. 2. – Lifetime of the Dy BEC when irradiated by the blue light without the second grating (green points) and with the second grating (purple points). The solid lines represent exponential fits. The inset shows the geometry of the measurement. The condensate is held in place by a dipole trap made by two crossing infrared lasers (shown in red) while the blue light hits the atoms along their magnetization axis.

3. – Characterization of the DMD

3·1. *The digital micromirror device.* – A Digital Micromirror Device (DMD) is a reflecting spatial light modulator made by an array of squared micromirrors that can control the intensity profile of an incoming light beam(2). By setting on the DMD's software a black and white image that has the same dimensions as the DMD board itself, this image will be displayed on the DMD board and can then be casted inside the light illuminating the DMD chip. This is done by assigning every entry of the matrix with its corresponding mirror. If a mirror is in the 0 (Off) state it means that it will be tilted in one way, whereas if it is in the 1 (On) state the micromirror will be tilted in another direction. The result of the different tilting of the mirrors will produce 2 different outgoing beams. One that is generated by the mirrors tilted in the Off state, and one beam generated by the On state mirrors. This creates the imprinting of the image sent to the DMD inside the "On" beam, whereas the "Off" beam contains a negative of this image. As can be seen in fig. 3(a), thanks to the DMD a ring can be casted inside the light source.

3·2. *Simulations of the superfluid to supersolid phase transition in the ring.* – To check if the experimentally achieved rings are free enough from defects and aberrations to make the superfluid delocalize inside the ring and to achieve an evenly spaced supersolid we made numerical simulations. We use the imaginary time evolution method to find the ground state of the extended Gross-Pitaevskii Hamiltonian(3)

$$H = \left(-\frac{\hbar^2\nabla^2}{2m} + V_{h.o.}(\boldsymbol{r}) + V_{ring}(x,y) + g|\psi(\boldsymbol{r})|^2 + V_{dd}^{mf}(\boldsymbol{r}) + \gamma(\epsilon_{dd})|\psi(\boldsymbol{r})|^3\right), \quad (1)$$

(2) The DMD that has been characterized in this work is the "DLP65000 0.65 1080p MVSP Type A" by Texas Instruments.
(3) More information on the extended Gross-Pitaevskii equation can be found in [15].

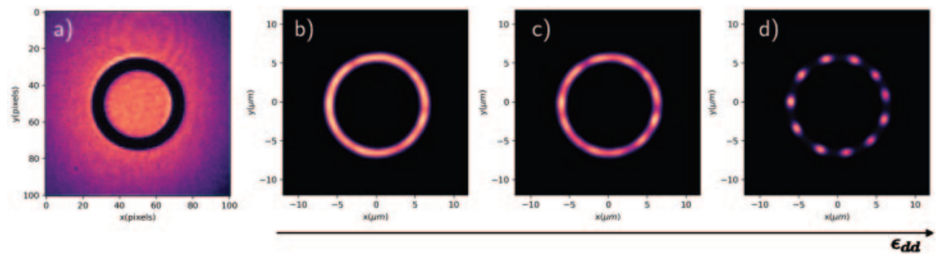

Fig. 3. – (a) Image of a ring casted inside the laser spatial profile after impinging on the DMD. The ring radius r at this stage is around $70\,\mu$m while its thickness δ is around $30\,\mu$m. This ring will then be demagnified on the atomic plane by a microscope to have final dimensions of $r \sim 5\,\mu$m and $\delta \sim 2\,\mu$m. (b)–(d) Superfluid to supersolid phase transition simulated inside the experimentally generated ring potential. The transition occurs when the parameter ϵ_{dd}, describing the ratio of dipolar and contact interaction, crosses a critical value.

where in this equation $V_{h.o.}(\boldsymbol{r}) = m(\omega_x^2 x^2 + \omega_y^2 y^2 + \omega_z^2 z^2)/2$ represents an harmonic confinement term, $g = 4\pi\hbar^2 a_s/m$ represents the strength of the contact interaction, a_s being the s-wave scattering length. $V_{dd}^{mf}(\boldsymbol{r}) = \int \mathrm{d}\boldsymbol{r}' V_{dd}(\boldsymbol{r} - \boldsymbol{r}')|\psi(\boldsymbol{r}')|^2$ represents the mean field contribution of the magnetic dipole-dipole interaction, V_{dd} being the dipole-dipole potential. The beyond mean field term $\gamma(\epsilon_{dd})|\psi|^3$ is inserted to study the onset of supersolidity. Lastly, inside eq. (1) the term $V_{ring}(x, y)$ represents the confining ring experimentally generated through the use of the DMD. This is just a recorded picture of the DMD ring similar to the one shown in fig. 3(a). Since the ring will have a radius of $5\,\mu$m in the atomic plane, the dimensions of the image are adjusted to make it this size. Moreover, the intensity of the image, that in the camera is a 8-bit number, is converted to an energy, to make the ring potential have an average height of about 200 nK. The simulations are done with a total atom number $N = 50 \times 10^3$ and an harmonic potential characterized by $(\omega_x, \omega_y, \omega_z) = 2\pi(20, 20, 100)$ Hz. This potential traps the atoms in the z direction against gravity and in the experiment will be realized through an optical light sheet made by a green laser that is already present in the experiment. The simulations are performed changing the parameter ϵ_{dd} describing the ratio of dipolar and contact interaction. When this parameter becomes bigger than a critical value (that depends on the number of atoms and on the trap geometry) the superfluid to supersolid quantum phase transition occurs. In fig. 3(b)–(d) the results of these simulations are shown. From these simulations we obtain both a superfluid ground state that is completely delocalized inside the ring and an evenly spaced supersolid. We can then infer that the ring potential realized with the DMD is good enough to see the delocalization of the superfluid and the formation of the supersolid in our ring.

4. – Conclusions

In conclusion, I reported the work made towards the realization of an annular potential, where in the near future we will trap a dysprosium BEC. This potential will completely change the symmetry of our system and will allow us to address interesting phenomena such as persistent currents and to tackle the question of how a supersolid behaves when put under rotation.

* * *

The author thanks the dysprosium Florence-Pisa group for the work done together.

REFERENCES

[1] Tanzi L. *et al.*, *Phys. Rev. Lett.*, **122** (2019) 130405.
[2] Chomaz L. *et al.*, *Phys. Rev. X*, **9** (2019) 021012.
[3] Böttcher F. *et al.*, *Phys. Rev. X*, **9** (2019) 011051.
[4] Tanzi L. *et al.*, *Nature*, **574** (2019) 382.
[5] Tanzi L. *et al.*, *Science*, **371** (2021) 1162.
[6] Biagioni G. *et al.*, *Science*, **371** (2021) 1162.
[7] Norcia M. A. *et al.*, *Nature*, **596** (2021) 357.
[8] Sohmen M. *et al.*, *Phys. Rev. Lett.*, **126** (2021) 233401.
[9] Sohmen M. *et al.*, *Nature*, **574** (2019) 386.
[10] Tengstrand, M. *et al.*, *Phys. Rev. A*, **103** (2021) 013313.
[11] Ryu C. *et al.*, *Phys. Rev. Lett.*, **99** (2007) 260401.
[12] Del Pace G. *et al.*, *Phys. Rev. Lett.*, **106** (2011) 130401.
[13] Del Pace G. *et al.*, *Phys. Rev. X*, **12** (2022) 041037.
[14] Preti N., *Towards dipolar quantum gases in a ring*, Master Thesis, University of Florence (2023) available at `https://quantumgases.lens.unifi.it/publications/theses`.
[15] Wachtler F. *et al.*, *Phys. Rev. A*, **93** (2016) 061603.